Chalcogenide Letters Vol. 14, No. 11, November 2017, p. 465 - 474

EFFECT OF REACTION TEMPERATURE AND REACTION TIME ON THE PROPERTIES OF Cu_2ZnSnS_4 NANOCRYSTALLINE THIN FILMS PREPARED BY MICROWAVE IRRADIATION

Q. LI[a], A. X. WEI[a,b*], W. K. TAO[a], J. LIU[a], Y. ZHAO[a], Z. M. XIAO[a]
[a]*Guangdong Provincial Key Laboratory of Functional Soft Condensed Matter, School of Material and Energy, Guangdong University of Technology, Guangzhou 510006, China*
[b]*Department of Information Science，Xin Hua College of Sun Yat-Sen University, Guangzhou 510520，China*

In this paper, Cu_2ZnSnS_4 (CZTS) nanocrystalline thin films were directly grown onto the FTO conductive glass by microwave-assisted solution method. The influences of reaction temperature and reaction time on the crystallographic structure, morphology and optical properties of CZTS thin films were investigated using X-ray diffraction, Raman spectroscopy, scanning electronic microscope and UV-Vis spectrophotometer. Results revealed that the as-synthesized thin films are mainly composed of CZTS phase with kesterite crystal structure; however it contains a little binary and ternary impurities phase of ZnS, SnS, $Cu_{2-x}S$ and Cu_2SnS_3. The CZTS nanocrystalline thin films are a number of composed of sphere-like particles and have an optical band gap 1.32-1.58 eV. The reaction temperature and reaction time have obvious influence to diameter and density of sphere-like particles, as also as optical band gap. The optimal reaction temperature and reaction time are 190-200°C and 60-90min for the synthesis of high-quality CZTS thin films by microwave irradiation method.

(Received September 1, 2017; Accepted November 2, 2017)

Keyword: Solar energy materials, Cu_2ZnSnS_4, Thin films, Microwave synthesis

1. Introduction

Low cost, high efficiency and less environmental pollution have been regarded as the indispensable properties for the next generation solar cells materials. Among various types of solar cells, the $CuIn_xGa_{1-x}Se_2$ (CIGS) thin film solar cell has attracted great interest for its high power conversion efficiency and stability [1, 2]. Nevertheless, gallium and indium are rare and expensive element, which impede the development of CIGS thin film solar cells. Fortunately, researchers found that copper zinc tin sulfide (Cu_2ZnSnS_4, CZTS) is a commendable photon absorber material to replace CIGS [3]. Cu_2ZnSnS_4 is a direct band-gap p-type semiconductor which has large absorption coefficient (~10^4 cm^{-1}) in visible region, optimal band-gap energy (~1.5 eV), good photostability and high photocorrosion resistance in air and aqueous solution. Recently, it has been reported that a non-vacuum deposition route led to a record of 11.2% power conversion efficiency for CZTS-based thin film solar cells [4], while theoretically predicted efficiency for CZTS-based solar cells can be up to 32.2% [5]. Therefore, a lot of work can be done in order to bring the power conversion efficiency closer to the theoretical limit. At present, many vacuum deposition methods have been adapted to fabricate CZTS thin film, such as sputtering [6], pulsed laser deposition [7] and chemical vapor deposition [8]. Solution-based synthesis of CZTS offers a low cost and high throughput alternative to vacuum-based methods. Several solution-based approaches to synthesize CZTS have been researched, such as the spray pyrolysis [9], the so-gel method [10, 11],

*Corresponding author: weiax@gdut.edu.cn

microwave-assisted solution methods [12-15], hot-injection solution synthesis method [16] and solvothermal method [17, 18]. Among those methods, microwave irradiation is an established technique for the controlled synthesis of various nanomaterials for its advantages like favorable homogeneity, shorter crystallization time, improved yield, better size control, good purity and reproducibility. Those advantages distinguish microwave irradiation a rapid and efficient method from the various vacuum and no vacuum methods. Microwave irradiation produces efficient internal heating by direct coupling of microwave energy with the reactant, which signally reduces the reaction times. Hence, the conductive films are selectively heated by microwave energy, resulting in selective deposition of target materials by thermolysis. Recently, there are several reports about the preparation of CZTS powders by microwave irradiation [14, 19-20]. Furthermore, Knutson has done pioneering work on the synthesis of CZTS thin films directly onto FTO glass substrates through microwave irradiation in 2014 [21]. Generally speaking, the CZTS films used as the absorbers layers of solar cell can be obtained by printing, spraying, or dip-coating the CZTS particles onto larger area substrates [22]. The influence of synthesis conditions on the properties of CZTS particles has been studied previously. Shin et al. reported the critical effect of Cu concentrations on the synthesis of single phase CZTS nonocrystals [23]. Wang et al. reported the effects of sulfur sources on the morphology and size of the CZTS nanoparticles [24]. Chen et al. and Wang et al. studied the influences of the reaction temperature on the chemical composition and phase purity of CZTS nonocrystals [25, 26]. However, it is necessary to further research controlled growth and growth mechanism of CZTS thin films.

In this paper, the successful and rapid synthesis of CZTS thin films onto conductive substrates by microwave irradiation is reported. The influence of reaction temperature and reaction time on the phase purity, crystallographic structure, morphology and optical property of the CZTS nanocrystalline thin films were studied in detail.

2. Experimental details

2.1. Microwave synthesis of CZTS nanocrystalline thin films

The CZTS nanocrystalline thin films were grown directly onto the FTO substrate using microwave assisted solution method. All the reagents are of analytical grade. Copper (II) chloride dihydrate ($CuCl_2{\cdot}2H_2O$), zinc (II) chloride dihydrate ($ZnCl_2{\cdot}2H_2O$), tin (II) chloride dihydrate ($SnCl_2{\cdot}2H_2O$), thiourea (NH_2CSNH_2) and ethylene glycol were used as starting materials. The FTO glass substrate was ultrasonically cleaned for 10 min in acetone, alcohol and de-ionized water successively, and then dried in air. In a typical synthesis process, 0.008mol of $CuCl_2{\cdot}2H_2O$, 0.004mol of $ZnCl_2{\cdot}2H_2O$, 0.004mol of $SnCl_2{\cdot}2H_2O$, 0.018mol of NH_2CSNH_2 were added to the 100ml of ethylene glycol as the precursor solution and then stirred the mixture for 10min. The well-cleaned FTO substrate was placed against the wall at an angle in a flask. When the reactant had been dissolved completely in the ethylene glycol, the solution was transferred into the flask and then placed the flask in a 2.45 GHz Xinhua XH-100A microwave reactor. The microwave heating was operated at a power of 700 W and temperature of 200℃ for 1 h. After the reaction, the microwave power was turned off and the sample was cooled down to room temperature by air flow. The samples were taken out and washed with de-ionized water for several times and dried in the ambient. Two series of samples were prepared to investigate the effect of reaction temperature and reaction time on the phase purity, crystallographic structure, morphology and optical property of the CZTS nanocrystalline thin films. The deposition parameters for various samples are listed in Table 1.

Table 1. Parameters of deposition process for various samples

Sample No.	$CuCl_2•2H_2O$ mol	$ZnCl_2•2H_2O$ mol	$SnCl_2•2H_2O$ mol	$CS(NH_2)_2$ mol	$(CH_2OH)_2$ ml	Temperature ℃	Power W	Time min
A1	0.008	0.004	0.004	0.018	100	170	700	60
A2	0.008	0.004	0.004	0.018	100	180	700	60
A3	0.008	0.004	0.004	0.018	100	190	700	60
A4	0.008	0.004	0.004	0.018	100	200	700	60
B1	0.008	0.004	0.004	0.018	100	200	700	30
B2	0.008	0.004	0.004	0.018	100	200	700	60
B3	0.008	0.004	0.004	0.018	100	200	700	90
B4	0.008	0.004	0.004	0.018	100	200	700	120

2.2. Characterization of CZTS nanocrystalline thin films

The crystallographic structure and phase purity of the as-synthesized CZTS thin films were identified by the X-ray diffractometer (XRD, D/MAXUltimaⅣ, Rigaku) using a CuK_α radiation source (λ= 0.1542 nm), over diffraction angles ranging from 20° to 80° at a scanning speed of 6° min^{-1} with a grazing angle of 0.5°. The phase purity of the products was further characterized using a Raman spectrometer (Renishaw, 514.5nm) accompanied by an Ar ion laser (λ = 514.5 nm) as an excitation source. The morphology of the CZTS thin films was analyzed using scanning electron microscopy (SEM, S-3400N, Hitachi). The optical properties of the CZTS thin films were investigated employing a UV–Vis–NIR spectrophotometer (T6) in the wavelength range of 400–1100 nm.

3. Results and discussion

3.1. Effect of reaction temperature on property of CZTS nanocrystalline thin films

The XRD patterns of CZTS nanocrystalline thin films prepared at different reaction temperature were shown in Fig.1 (a). Besides those characteristic peaks from FTO substrate (marked by ♣), the major XRD diffraction peaks appeared at 28.52°, 47.30°, 56.23° are corresponding to (112), (220) and (312) planes of kesterite crystal structure with cell parameters a=b=0.5427 nm, c=1.0848 nm (JCPDS NO.26-0575). Even if reaction temperature were increased from 170° to 200°C, the XRD patterns of CZTS thin films have no obvious change, as seen in Fig.1 (a). According to Debye–Scherer equation based on the (112) peaks of XRD patterns, the average crystallite sizes of CZTS thin films can be calculated. And they are 6.75 ± 1.6 nm, 7.71± 1.6 nm, 7.73 ± 1.6 nm and 7.58 ± 1.6 nm for samples prepared at temperature of 170 °C, 180 °C, 190°C and 200°C, respectively. In calculating the crystallite sizes, the value of Scherer constant K is taken as 0.94. The results indicated that the grain size of crystallite slightly increases with the increasing of reaction temperature.

In XRD patterns of Fig.1 (a), besides those characteristic peaks from CZTS thin films and FTO substrate, a lot of diminutive peaks （marked by ↓） at 23.62°, 30.38°, 35.7°, 40.3°, 42.23°, 43.9°, 49°, 54.7°, 64.16°, 69.27° and 73.28° are scrutinized. In spite of the intensity of these diminutive peaks is very weak comparing to peak of kesterite (112) at 28.53°. These additional peaks are probably because of the presence of binary and ternary phases, such as ZnS, SnS_2, $Cu_{2-x}S$, Cu_3SnS_4 and so on. Although XRD is generally used to analyze the structure of such compounds, it is not sufficient to identify most of the minor phases, since cubic ZnS (JCPDS No. 5-0566) and tetragonal Cu_2SnS_3 (JCPDS No. 89-4714) have very similar diffraction pattern with tetragonal CZTS. Therefore, Raman spectroscopy was used to further confirm the phase purity of

as-synthesized CZTS thin films. Fig. 1(b) shows the Raman spectra of CZTS thin films synthesized at different reaction temperature. The Raman spectrum of CZTS thin films synthesized at 170-200℃ exhibits two strong peaks at 332cm^{-1} and 290 cm^{-1}, which can be attributed to the kesterite structure CZTS [27]. Meanwhile, the weak peaks at 250 cm^{-1}, 317 cm^{-1} 425 cm^{-1} and 475cm^{-1} also were observed for CZTS thin films prepared at 170℃and 180℃. Only the weak peak at 317cm^{-1} were observed for samples grown at 190℃ and 200℃. As seen in Fig. 1(b), the broad peaks centered at around 290 cm^{-1} and 332 cm^{-1} can be considered as the superimposed spectrums of tetragonal CZTS (290cm^{-1} and 332 cm^{-1} [27, 28]), tetragonal Cu_2SnS_3 (297cm^{-1} and 352 cm^{-1} [27, 28]) , and orthorhombic Cu_2SnS_3(318 cm^{-1}). The peak at 250cm^{-1} and 475 cm^{-1} can be assigned $Cu_{2-x}S$ [27, 28]. According to the results of XRD and Raman data, the CZTS thin films prepared by microwave-assisted solution method are mainly composed of CZTS, however it contains a little binary and ternary impurities phase of ZnS, SnS, $Cu_{2-x}S$ and Cu_2SnS_3.

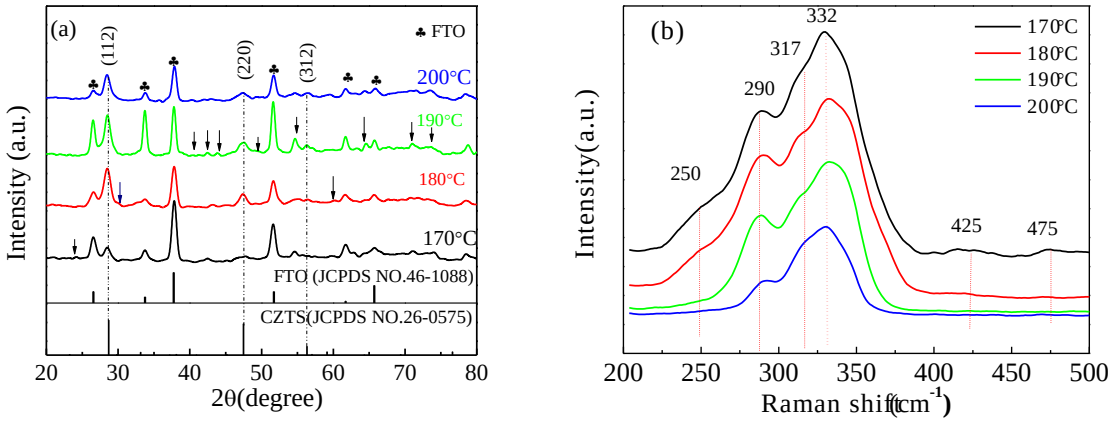

Fig. 1 (a) X-ray diffraction pattern and (b) Raman spectrum of the CZTS thin films prepared at different reaction temperature

The SEM images of the as-synthesized CZTS nanocrystalline thin films prepared at different temperature are shown in Fig. 2. As seen from Fig.2, the CZTS thin films are mainly composed of a number of sphere-like particles, and the average diameter of sphere-like particles is 150±10 nm,150±10 nm ,140±10 nm and 310±10 nm for samples synthesized at 170°C,180°C,190 °C and 200°C, respectively. However, for sample prepared at 180°C, thin films are composed of both sphere-like particles and sheet-like flakes. The emergence of sheet-like flakes needs further analysis. In addition, the density of the sphere-like particles for thin films prepared at 190°C is denser than that for the other three samples. Hence, the reaction temperature has influence to the compactness and average size of sphere-like particles. Base on the above results, the optimum temperature used in the process of microwave irradiation should be 190℃.

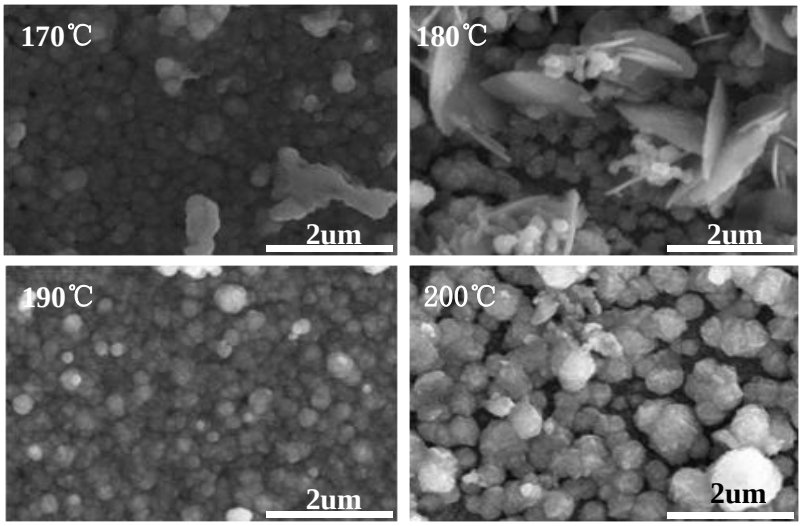

Fig. 2. SEM of the CZTS thin films prepared at different reaction temperature

In order to verify the composition of the thin films, the elemental analysis of the as-synthesized CZTS thin films was performed using the EDS technique. The contents of Cu, Zn, Sn, S and atomic ratios Cu/Zn, S/Cu of various samples are listed in Table 2. Although the amounts of thiourea are 2.25 times of copper (II) chloride dihydrate in precursor solution, the S content of CZTS thin films is much lower than the ideal target value. Compared Cu content with Zn content, the Cu content of CZTS thin films is much higher than the ideal target value. The Cu: Zn: Sn: S atomic ratios deviated from the theoretical value of 2:1:1:4 of stoichiometric Cu_2ZnSnS_4. The Sn content contained in FTO substrate may result in the high concentration of Sn in the CZTS thin films. As seen from XRD patterns of CZTS nanocrystalline thin films, the presence of a little $Cu_{2-x}S$ and Cu_3SnS_4 in CZTS thin films is another possible reason for the high Cu and Sn content. In addition, the slightly Sn rich and Zn poor composition may be ascribed to the reactivity of different metal precursor. Since the Zn source shows lower reactivity than the Cu and Sn sources, the reagents contain more Zn salt than the stoichiometric amount for the expected cation ratios. Seen from Table 1 and Table 2, the reaction temperature affect the Cu/Zn, S/Cu and Cu/Zn/Sn/S atomic ratio of CZTS thin films, although the concentration of Cu , Zn , Sn, S salts and other experimental conditions are exactly the same. The ideal stoichiometry of CZTS requires that the atomic ratios of Cu/ (Zn+Sn) and Zn/Sn equal to 1. However, Katagiri et al [29] suggest that the atomic ratios of Cu/ (Zn+Sn) and Zn/Sn near to 0.85 and 1.25 respectively show good optoelectronic properties and best device efficiency.

Table 2 Atom ratios of CZTS thin films prepared using different temperature

Sample No	Cu at%	Zn at%	Sn at%	S at%	Cu/Zn	S/Cu	Cu/Zn/Sn/S
A1	26.3	11.1	31.9	30.5	2.37	1.16	2.4:1:2.9:2.7
A2	30.0	11.3	22.0	36.6	2.65	1.22	2.7:1:1.9:3.2
A3	25.7	10.4	30.5	33.7	2.47	1.31	2.5:1:2.9:3.2
A4	30.1	10.6	25.3	33.9	2.84	1.13	2.8:1:2.4:3.1

UV-vis transmission spectroscopy of the CZTS thin films prepared at different reaction temperature is shown in Fig.3 (a). Except for sample A1, the transmission of the CZTS thin films is less than 50% in range of 400nm-900nm wavelength, demonstrating that the CZTS thin films has better capacity of light absorption. Therefore, CZTS thin films are suitable to be served as the absorption layer of the solar cells. The values of the absorption coefficient α of the CZTS thin films could be calculated by analyzing the transmission spectra using formula as following:

$$\alpha = \frac{1}{d}\ln(\frac{1}{T}) \tag{1}$$

The thickness d of the thin films is determined from cross-sectional view of SEM images. T is transmittance of the thin films. Because CZTS is direct-band-gap semiconductor, the relationship between absorption coefficient α and the incident photon energy hν can be expressed using the Tauc relationship:

$$(\alpha h\nu)^2 = A(h\nu - E_g) \tag{2}$$

Where A is a constant, E_g is the optical band gap energy. Relation (2) can be further written as the following form:

$$(\alpha h\nu)^2 = A(h\nu - E_g) \tag{3}$$

The corresponding plots of $(\alpha h\nu)^2$ as a function of hν is shown in Fig.3 (b). Extrapolation of the linear portion of the curves to $(\alpha h\nu)^2 = 0$ gives the optical band gap E_g. The values of the optical band gap are1.32±0.01 eV, 1.34±0.01 eV, 1.36±0.01 eV, 1.38±0.01 and 1.57±0.01 eV for sample A1, A2, A3 and A4, respectively. The optical band gap of CZTS thin films varied in the range 1.32-1.57 eV due to the existence of impurities in the samples and their amount varies sample by sample. Since the presence of secondary phases like Cu_2SnS_3 (0.96eV), ZnS (3.6eV) SnS (2.05eV) will decrease and increase the band gap of the synthesized CZTS thin films, respectively. The band gap of 1.5 eV is equal to the optical gap of the CZTS thin films. The strong absorption in the visible light region and band gap of approximately 1.5 eV is suitable to work as absorber layer of thin film solar cells.

Based on analysis of XRD, SEM and optical gap results, the optimal reaction temperature is 190-200°C. Note that the boiling point of ethylene glycol is 197.3℃; therefore we conducted our experiment at temperature no higher than 200℃.

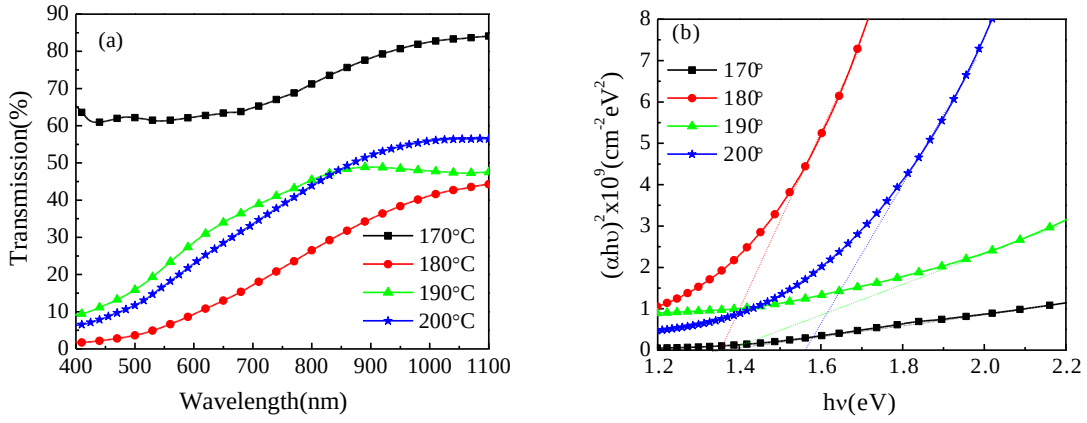

Fig. 3 (a) UV-vis transmission spectroscopy and (b) $(\alpha h\nu)^2$-$h\nu$ curves of CZTS thin films prepared at different reaction temperature

3.2. Effect of reaction time on properties of CZTS nanocrystalline thin films

Fig. 4(a) shows the XRD pattern of the CZTS thin films prepared at 200℃ for reaction time of 30min, 60min, 90min and 120 min, respectively. Except for those characteristic peaks from FTO substrate, the major XRD diffraction peaks of all the four samples appeared at 28.51°, 47.29°, and 56.23°can be indexed (112), (220) and (312) planes of the kesterite crystal structure(JCPDS NO.26-0575). The weak diffraction peaks appeared at 2θ=42.7° and 54.8° are observed, and they result from impurities phase. The reaction time on the result indicated that the as-synthesized thin films are mainly composed of CZTS with kesterite crystal structure, however it contains the a little secondary phase. The average crystallite sizes calculated using Debye-Scherer equation based on the (112) peaks of XRD patterns are 6.75nm ± 1.6 nm, 7.58nm ± 1.6 nm, 7.85nm ± 1.6 nm and 8.73nm ± 1.6 nm for samples prepared for duration of 30min, 60min, 90min and 120 min, respectively. The average crystallite sizes of CZTS nanocrystalline thin films increases with the increasing of the reaction time. Fig. 4(b) shows the Raman spectra of the CZTS thin films prepared at 200℃ with reaction time of 30min, 60min, 90min and 120 min, respectively. All samples show two strong peaks at 290 cm^{-1} and 332 cm^{-1} and it is accomplished by weaker peaks at 250 cm^{-1} and 475cm^{-1}. The broad peaks centered at around 290 cm^{-1} and 332 cm^{-1} could be considered as the characterize peaks of tetragonal CZTS, and the peaks at 250cm^{-1} and 475 cm^{-1} could be assigned $Cu_{2-x}S$.

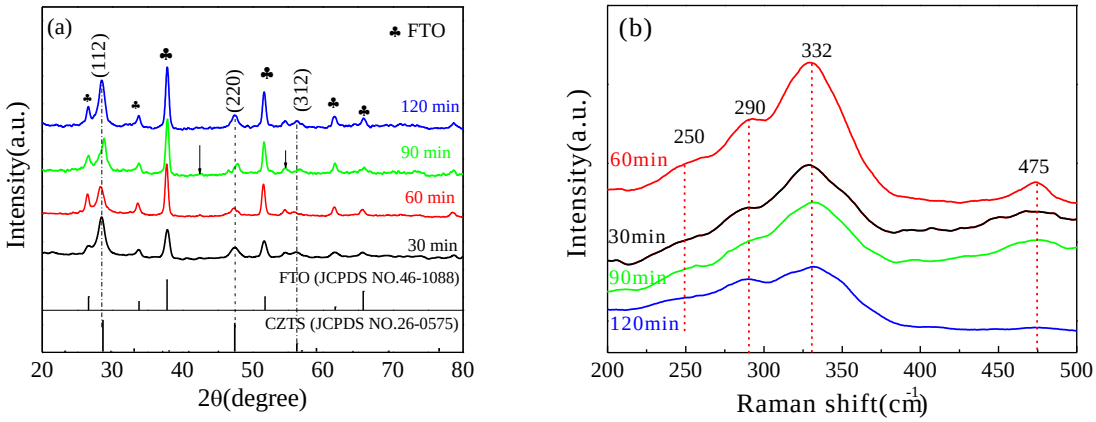

Fig. 4 (a) X-ray diffraction pattern and (b) Raman spectrum of the CZTS thin films prepared at different reaction time

Fig. 5 shows the SEM images of CZTS thin films grown on the FTO substrate with growth time of 30min, 60min, 90min and 120 min while the reaction solution and reaction temperature are kept the same for all samples. Regardless of the growth time, the CZTS films are composed of large sphere-like particles. However, the diameter of the sphere-like particles decrease, and the CZTS films become more densely packed with prolonging growth time. Hence, reaction time of CZTS thin films with high purity kesterite phase should be not less than 90 min.

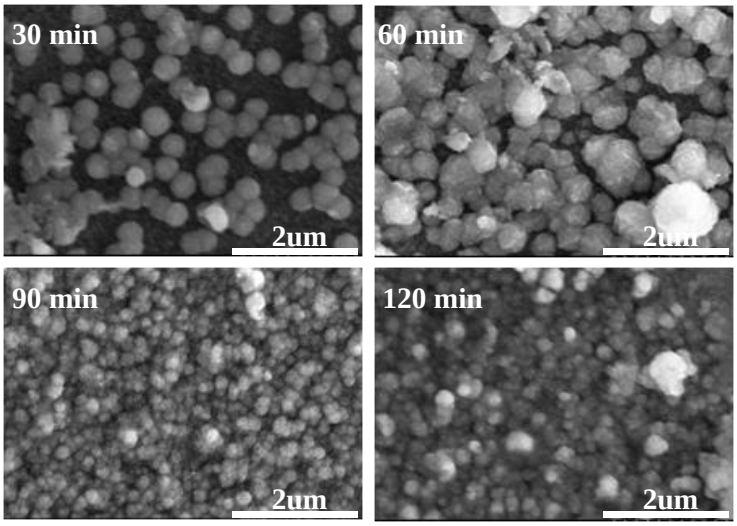

Fig. 5. SEM of CZTS thin films prepared at different reaction time

Fig.6 (a) presents the transmission spectra in the wavelength range of 400 nm to 1100 nm of the CZTS thin films deposited on the FTO substrate with growth time of 30min, 60min, 90min and 120 min, respectively. The transmission of the CZTS thin films is less than 50% in range of 400nm-900nm wavelength, demonstrating that the CZTS thin films has better capacity of light absorption. The optical band gap E_g is determined by extrapolating the linear portion of the curve to $(\alpha h\nu)^2 = 0$ as shown in Fig.6 (b) which is corresponding to the optical transmission spectra in Fig. 6(a). The optical band gap of CZTS thin films prepared with growth time of 30min, 60min, 90min and 120 min is 1.35±0.01 eV, 1.49 ±0.01eV, 1.50±0.01eV, 1.58±0.01eV respectively. The energy gap of CZTS thin films prepared at 60min and 90min is closed to the optimal optical band gap of solar cells, therefore the optimal reaction time is 60-90min for synthesis of CZTS thin films.

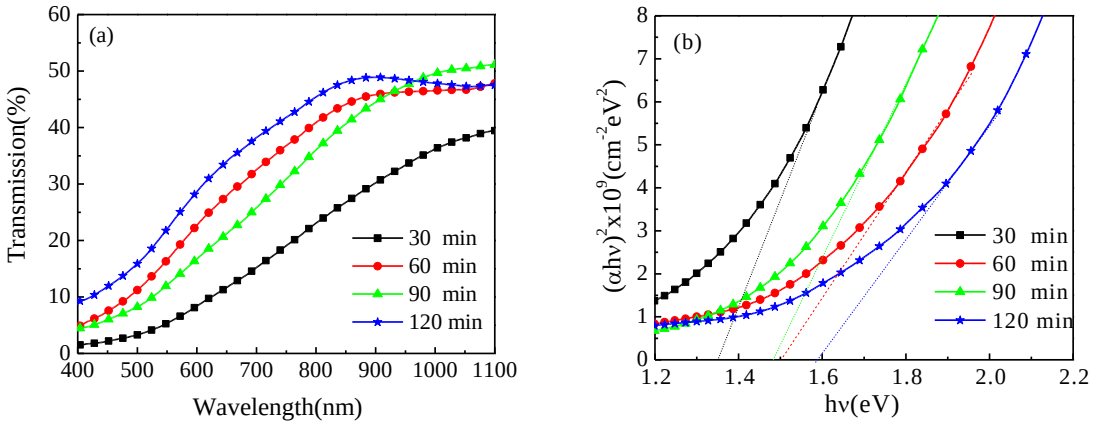

Fig. 6. (a) UV-vis transmission spectroscopy and (b) $(\alpha h\nu)^2$-$h\nu$ curves of CZTS thin films prepared at different reaction time

3.3. Growth mechanism of the CZTS thin film on FTO substrate

On the basis of the above results, the growth mechanism of microwave synthesis of CZTS thin films can be proposed as shown in Fig.7. Actually, the whole formation process of CZTS thin films involves three steps. In the First step, Cu^{2+}, Zn^{2+}, and Sn^{4+} coordinate with thiourea (Tu)

molecules to form M-thiourea complexes ($[Cu(Tu)_n(H_2O)_x]^{2+}$ (Cu-Tu), $[Zn(Tu)_n(H_2O)_x]^{2+}$ (Zn-Tu) and $[Sn(Tu)_n(H_2O)_x]^{4+}$ (Sn-Tu) in reaction solvent. When all reagents were dissolved, mixed and stirred in ethylene glycol, the colors of the precursor solution change from pea green to colorless transparent solution, which confirms the formation of metal-thiourea (Tu) complexes. Secondly, when FTO substrates were immersed in the precursor solution and irradiated with microwave energy, CZTS thin films were deposited only on the conductive side of substrates, there were no CZTS thin films on nonconductive sides of the substrates. However，there is some nanoparticles precipitation in reaction solution. With prolonging time of microwave irradiation, the color of the reaction solution turned from light green to brown and finally black. Under microwave irradiation conditions, the Cu-Tu complexes firstly decomposed to $Cu_{2-x}S$ nucleus for its strong ability of absorb microwave, which can grow in the preferred orientation and formed lamellar particles. Meanwhile, the Zn-Tu and Sn-Tu complexes decompose to ZnS and SnS, which react with $Cu_{2-x}S$. The copper sulfide nucleus which act as the starting point for the nucleation and growth of CZTS, gradually disappear and transform into CZTS grains. As the spherical structure conserves the lowest surface energy, the nucleuses grow into large grain by Ostwald ripening and aggregate together to form a spherical structure. The FTO was a polycrystalline films with a tetragonal structure, and had homogeneous surfaces with average grain size around 180 nm. It is expected that the suitable electrical conductivity and surface roughness may induce nucleation and growth of CZTS thin films. The microwave energy was strongly absorbed only by the thin conductive coating, preferentially heating it to temperatures high enough to enable selective thermolysis of precursors and deposition of CZTS directly onto the conductive coating.

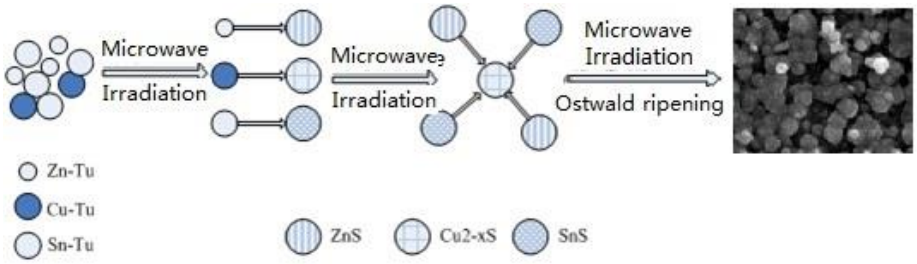

Fig.7. Schematic diagram of growth mechanism of the CZTS thin films prepared using microwave irradiation

4. Conclusions

In summary, the CZTS nanocrystalline thin films are successfully prepared on FTO substrates using the single-step microwave-assisted solution method. The influence of reaction temperature and reaction time on the phase purity, crystallographic structure, morphology and optical property of CZTS thin films were investigated, respectively. The CZTS thin films are in the kesterite structure with a little impurity phase. The CZTS thin films are composed of a large number of uniform sphere-like particles. Each sphere-like particle contains many nanocrystals that are approximately 7.5 nm in average crystallite size. The average crystallite sizes of CZTS nanocrystalline thin films increases with the increasing of the reaction time or reaction time.

The reaction temperature affects the compactness and average size of sphere-like particles. The optical band gap of CZTS thin films varied in the range 1.32-1.57 eV with increasing reaction temperature from 170℃ to 200 ℃. The reaction time does not obviously affect crystal structures, but markedly affect the surface morphology and the compactness of the CZTS thin films. Base on the above results, the optimal reaction temperature and reaction time are 190-200℃ and 60-90min for the synthesis of high-quality CZTS thin films by microwave irradiation method. The microwave-assisted solution method provides a promising route for the fast, low-cost and large-scale fabrication of the CZTS thin films.

Acknowledgements

We acknowledge the financial supports from the Science and Technology Program of Guangdong Province of China (No. 2016A010104020), the Training Plan of Outstanding Young T eachers of Universities in Guangdong Province (No. YQ2015055).

References

[1] P. Jackson, D. Hariskos, R. Wuerz, W. Wischmann, M. Powalla, Phys. Status Solidi Rapid Res. Lett. **8**, 219 (2014).
[2] T. Wada, S. Nakamura, T. Maeda, Prog. Photovolt. Res. Appl. **20**, 520 (2012).
[3] H. Katagiri, K. Jimbo, W.S. Maw, K. Oishi, M. Yamazaki, H. Araki et al., Thin Solid Films **517**, 2455 (2009).
[4] X. Song, X. Ji, M. Li, W. Lin, X. Luo, H. Zhang, Int. J. Photoenergy **2014**, 613173 (2014)
[5] W. Shockley, H.J. Queisser, J. Appl. Phys. **32**, 510 (1961).
[6] F. Liu, Y. Li, K. Zhang, B. Wang, C. Yan, Y. Lai et al., Sol. Energy Mater. Sol. Cells **12**, 2431 (2010).
[7] K. Moriya, K. Tanaka, H. Uchiki, Jpn. J. Appl. Phys. **46**, 5780 (2007).
[8] T. Washio, T. Shinji, S. Tajima, J. Mater. Chem. **22**, 4021 (2012).
[9] N. M. Shinde, R.J. Deokate, C.D. Lokhande, J. Anal. Appl. Pyrolysis **100**, 12 (2013).
[10] K. Zhang, J. Tao, J. He, J. Mater. Sci.: Mater. Electron. **25**, 2703(2014).
[11] G. L. Agawane, S.W. Shin, S.A. Vanalakar, J. Mater. Sci.: Mater. Electron. **26**, 1900 (2015).
[12] R. S. Kumar, B.D. Ryu, S. Chandramohan, J.K. Seol, S.K. Lee, C. H. Hong, Mater. Lett. 86, 174 (2012).
[13] W. Wang, H. Shen, F. Jiang, X. He, Z. Yue, J. Mater. Sci.: Mater. Electron. **24**, 1813 (2013).
[14] K. Wang, P. Chen, C. Tseng, CrystEngComm **15**, 9863 (2013).
[15] T.R. Knutson, P.J. Hanson, E.S. Aydilb, R.L. Penn, Chem.Commun. **50**, 5902 (2014).
[16] X.T. Lu, Z.B. Zhuang, Q. Peng, Y.D. Li, Chem. Commun. **47**, 3141 (2011).
[17] A. Wei, Z. Yan, Y. Zhao, M. Zhuang, J. Liu, Int. J. Hydrog. Energy **4**, 797 (2015).
[18] Y. L. Zhou, W.H. Zhou, M. Li, Y. F. Du, S. X. Wu, J. Phys. Chem. C **115**, 19632 (2011).
[19] R. S. Kumar, B. D. Ryu, S. Chandramohan, J. K. Seol, S. Lee, C. Hong, Mater. Lett. **86**,174 (2012).
[20] S.W. Shina, J. H. Hana, C.Y. Park, A.V. Moholkar, J.Y. Lee, J. H. Kim, J. Alloy. Compd. 516 (2012).
[21] T. R. Knutson, P. J. Hanson, E. S. Aydilb, R. L. Penn, Chem. Commun. **50**, 5902 (2014).
[22] Q. Guo, H.W. Hillhouse, R. Agrawal, J. Am. Chem. Soc. **131**, 11672 (2009).
[23] S.W. Shina, J. H. Han, C.Y. Park, S. Kim, Y.C. Park, G.L. Agawane et al. J. Alloys. Compd. **541**, 192 (2012).
[24] W. Wang, H. Shen, X. He, J. Li, J. Nanopart. Res. **16**, 2437 (2014).
[25] J. Chen, Q. Chen, H. Yuan, T. Wang, F. Zhou, X. Dou, S. Zhuang, J. Mater. Sci.: Mater. Electron. **25**, 873 (2014).
[26] W. Wang, H. Shen, H. Yao, J. Mater. Sci.: Mater. Electron. **26**, 1449 (2015).
[27] P. R. Ghediya, T. K. Chaudhuri, J. Mater. Sci.: Mater. Electron. 26, 1908 (2015).
[28] P. A. Fernandes, P. M. P. Salomé, A. F. Cunha, J. Alloy. Compd. **509,** 7600 (2011).
[29] H. Katagiri, K. Jimbo, W. S. Maw, Thin Solid Films **517**, 2455(2009).